Jurnal Teknologi

Full Paper

MOLECULAR DYNAMIC SIMULATION OF V176G MUTATION ASSOCIATED WITH GERSTMANN–STRÄUSSLER–SCHEINKER AT ELEVATED TEMPERATURE

Ashraf Fadil Jomah*, Mohd Shahir Shamsir

Bioinformatics Research Group, Faculty of Bioscience and Medical Engineering, Universiti Teknologi Malaysia, 81310 UTM Johor Bahru, Johor, Malaysia

*Corresponding author
ashraf_jomah@yahoo.com

Article history
Received
19 August 2015
Received in revised form
17 September 2015
Accepted
15 January 2016

Graphical abstract

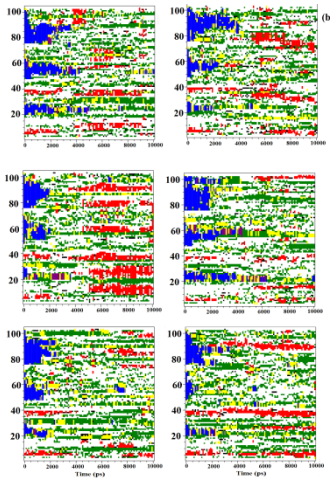

Abstract

The transformation of cellular prion protein (PrPc) into pathogenic conformer (PrPSc) in transmissible spongiform encephalopathy is expedited by mutations in the prion protein. One recently reported novel mutation V176G is located in region of the protein known to cause Creutzfeldt-Jakob disease (CJD) but possess a unique neuropathological profile and spongiform alteration similar to Gerstmann–Sträussler–Scheinker syndrome (GSS). Using molecular dynamics simulations; the denaturation of the prion structure with V176G at 500K was studied to identify the dynamics in structural properties such as salt bridge, solvent accessibility, hydrogen bonds and hydrophobicity. The simulations revealed that the heat-induced unfolding caused destabilization of the native structure of PrP and affecting the β-sheet region of the structure more than the a-helix. Unique salt bridge formation suggests conformational orientation that may be attributed to the V176G mutation. The mutation effects showed an increased fluctuation of the H1 region, gain of hydrogen bonds between H3 and H2 which may be part of the oligomerization pathway and determine the features of the PrPSc assemblies.

Keywords: Prion, Creutzfeldt-Jakob, Gerstmann-Sträussler-Scheinker, V176G, molecular dynamic simulations

Abstrak

Transformasi protin selular prion (PRPC) ke dalam bentuk patogenik (PrPSc) yang menjangkitkan penyakit spongiform encephalopathy disebabkan oleh mutase. Satu mutasi baru V176G terletak di bahagian protin menyebabkan penyakit Creutzfeldt-Jakob (CJD) tetapi mempunyai profil neuropatologi yang unik dan gugusan yang sama dengan sindrom Gerstmann-Sträussler-Scheinker (GSS). Dengan menggunakan simulasi dinamik molekul; struktur prion dengan mutase V176G di uji di suhu 500K untuk mengenal pasti perubahan dinamik struktur seperti jambatan garam, akses pelarut, ikatan hidrogen dan sifat nyahair. Simulasi menunjukkan bahawa suhu 500K menyebabkan ketidakstabilan struktur asal PrP dan memberi lebih kesan kepada kepingan β struktur berbanding a-heliks. Pembentukan unik jambatan garam mengusulkan orientasi structur baru yang diakibatkan oleh V176G. Kesan mutasi ketidakstabilan meningkat di H1, pertambahan ikatan hidrogen antara H3 dan H2 yang mungkin boleh menjadi punca terjadinya oligomer dan menentukan ciri-ciri gugusan penyakit PrPSc.

Kata kunci: Prion, Creutzfeldt-Jakob, Gerstmann-Sträussler-Scheinker, V176G, simulasi dinamik molekular

1.0 INTRODUCTION

Transmissible spongiform encephalopathy diseases caused by prions are a variety of degenerative disorders of the nervous system that can develop spontaneously or due to horizontal or vertical transmission and ultimately cause the death of the patient [2]. The development of prion disease is due to the aggregation of abnormally folded wild-type form of prion protein PrPc that is normally present in cells into the diseased PrPsc form. One of the differences between PrPc and PrPsc lie in their secondary structure content. PrPc has 42% helical (H) component in its structure and its beta sheet (β-sheet) content was extremely low 3%, whereas the percentage of helical component in PrPsc is 30% with beta sheet content of 43% [3, 4].

Recently discovered mutation V176G which was found in one patient in Spain in 2013. Post mortem study revealed a unique neurodegenerative condition which included deposition of amyloid plaques, degeneration of neurofibrillary tangles and emptiness in the brain as seen in Gerstmann- Straussler-Scheinker (GSS) [5]. However, the site of V176G mutation is located in regions commonly attributed to mutations that possess CJD symptoms (Figure 1).

Human familial prion diseases related to PrP originated from 40 point mutations and most of the mutations occur in the protein globular domain [1, 6]. These mutations are responsible for spontaneous generation of PrPSc in the brain [7]. The mutation's effect of thermodynamic instability in PrPC enhances the misfolding kinetics of PrP WT [8, 9] and the stability of partially folded intermediate species such as PrPSc precursors [10, 11]. The analysis of mutations carrying PrP provides significant insights into factors that increase the likelihood of misleading and induces different types of spontaneous prion diseases, even in the absence of infection from exogenous sources[12, 13].

The incidence of GSS is 1 in 100 million of population per year [28]GSS is genetically and phenotypically heterogeneous; multiple mutations in the prion protein (PRNP) gene result in various clinical symptoms which may show intrafamilial and intragenerational variation include chronic progressive ataxia, terminal dementia, a long clinical duration (2–10 yr), and multicentric amyloid plaques, dementia, dysarthria, ocular dysmetria, infrequent myoclonus, spastic paraparesis, parkinsonian signs, and hyporeflexia or areflexia in the lower extremities. The PRNP polymorphism M129V has been shown to influence the disease phenotype. When linked to V129 allele. Following PRNP mutations have been shown to cosegregate with GSS: P102L, P105L, A117V, Y145X, Q160X, F198S, Q217R, Y218N, Y226X and Q227X 211 [14, 15]This study, to assess differences in the properties and dynamics of the wild type and novel mutation (V176G) to gain more insights by compared in the high temperature level. In this study we used denaturing molecular dynamics simulations to investigate the effect of the point mutations on the stability by examining the unfolding of the protein chain. The mechanism of changes in protein structure have been attributed to protein denaturation that place at raised temperatures [16, 17]. It has also been discovered that increasing temperatures can also increase the rate of protein unfolding without any modification in the mechanism of unfolding [18, 19]. The changes in protein configuration can be researched upon by using simulation models based on molecular dynamics (MD) as it can not only replicate the environmental conditions needed for inducing change in protein structure but can also show the changes unfolding in real time. The results will provide investigate the influence of the unfolding of human prion protein which is important in the transition from the normal to abnormal form of the protein and mutation associated with induced temperature.

2.0 EXPERIMENTAL

The mechanism of changes in protein structure has been attributed to protein denaturation that place at raising temperatures [16, 17] . Recently, it has also been discovered that increasing temperatures can also increase the rate of protein unfolding without any modification in the mechanism of unfolding [18, 19]. The changes in protein configuration can be researched upon by using simulation models based on molecular dynamics (MD) as it can not only replicate the environmental conditions needed for inducing change in protein structure but can also show the changes unfolding in real time. The effects of pressure, temperature, pH and mutations on the transformation of PrPc to PrPsc have been studied successfully using this model [20-22]. The mutation V176G and wild type (WT) counterpart are evaluated with the aim of studying their physicochemical and dynamic properties like hydrophobicity, solvent accessibility and salt bridges.

2.1 Mutant Structure Construction

The prion pathogenic mutant structure V176G was constructed using WT PrP (125-228) (PDB code:1QLX) from the Protein Data Bank (PDB) and substituting the relevant amino acid residue [5]. The numbering of the residues was standardized from 125–228 to 0–103 and the valine polymorphism are maintained for these mutants at codon-129 (Figure 2).

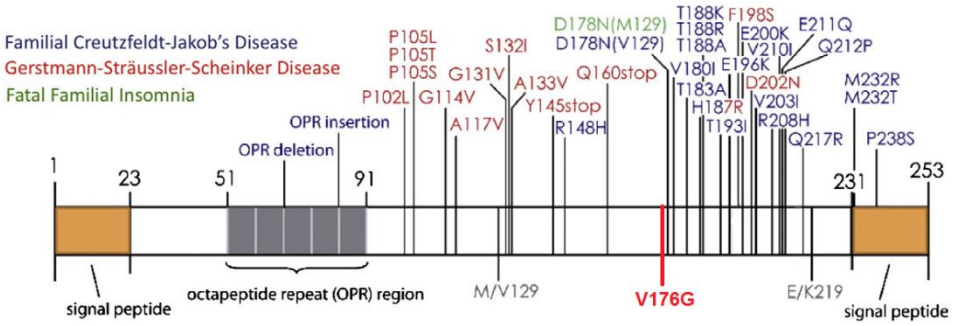

Figure 1 Location CJD, GSS and FFI mutation on the prion sequence. The CJD is coloured blue, GSS in red and FFI in green. The location of the novel mutation V176G is coloured bright red at the bottom of the diagram. The diagram is modified from [1]

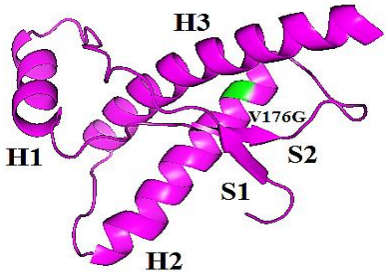

Figure 2 The globular domain of WT PrP (PDB ID: 1QLX) with the mutated residues V176G (green) created using PyMol

2.2 Molecular Dynamics Simulation

MD simulations are performed for 10 ns using GROMACS 4.6.3 package and all-hydrogen function GROMOS96. Test calculations involving multiple sets of independent MD simulations showed identical results. Hence, one single MD run of 10ns appears to be enough to reproduce the structural determinants of the MD [23]. All MD systems are simulated in the aqueous solution using a cubic box of water molecules with vector size 7.08 nm [24]. Neutral pH conditions are maintained according to their pKas by adjusting the protonation states of the ionisable residues, where Na ions are used as counter ions. Periodic boundary conditions in the NPT ensemble at a fixed temperature (T= 500 K) and pressure (P = 1 bar) are used via Nose`-Hoover and Andersen-Parrinello-Rahman coupling schemes. Long-range electrostatic interactions are treated within the Ewald particle mesh (PME) [25-28].

2.3 Simulation Analyses

All of the resulting trajectories are analysed using GROMACS utilities and results are recorded for a representative trajectory. The Ca root mean square deviations (RMSD) and its fluctuations (RMSF) relative to the average MD structure are computed. The structural evolution measured using the percentage of secondary structure throughout the simulations is determined using the DSSP program [29]. Images of protein structure and the electrostatic potential on the mutants surfaces are generated using Pymol [18, 30]. The VMD tool [30] software is employed to calculate the salt bridges in the range 4Aº.

3.0 RESULTS AND DISCUSSION

3.1 Conformational Changes and Overall Dynamics Behavior of the WT and Mutated PrP

RMSD values are estimated for the globular residues 125-228 in case of all simulations. Figure 3 depicts WT, V176G simulation as an example. Usually, the RMSD values are quite low in most simulations. It has also been seen that in certain mutant runs RMSD values decrease when compared to WT. The RMSD of V176G mutant is usually less than 1.5 nm in the last 2000 ns of the simulation. For V176G mutant runs the RMSD values increased like a higher RMSD values of 1.25 nm at 6000ns was seen for the mutant run 3. The values for root mean square fluctuations (RMSF's) were calculated for average structure in the designated time frame as they provide information about the strength of structural framework, structural modifications and structural flexibility that can be changed by mutations.

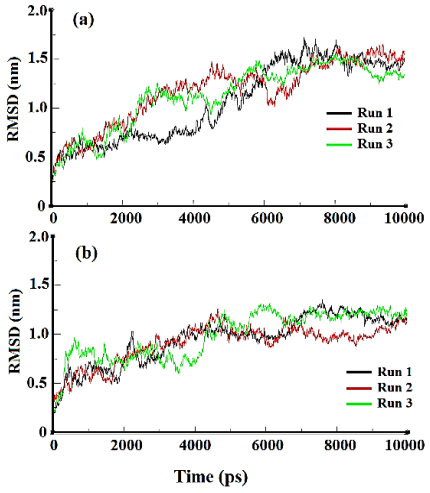

Figure 3 Ca RMSD obtained from the structure of the globular domain (residues 128–225) for PrP mutants (a) wild type, (b) V176G

Figure 4 shows the RMSF of mutated protein and WT so as to have a better understanding of structural changes. The prominent plateaus in RMSF graph showed high fluctuations due to the sum effect of fluctuations of loop 1 and loop 3, this was also noticed in past studies. NMR bundles had a high backbone displacement [31]. H2 and H3 which have a single disulphide bridge (C174-C214) show minimum fluctuation values. Mutations have changed RMSF values showing that H1 and H2 are unstable. It was also determined by NMR studies that loop between H2 and H3 had picoseconds time scale motions, loop before H1 (residues 137-141) had sub nanosecond flexibility and in loops around H2 and S2 there was a slow motion [32, 33]. These findings were in agreement with increased RMSF that was seen in the loop regions [31]. The WT variety of V176G more flexible and 205_215 are concerned [34] if compared to the WT, this difference is probably due to the different amino acids at the site of mutation. RMSF showed variation in loops between S1 and H1 and between H2 and H3 [31]. A study of the structural configuration has pinpointed the S2- H2 loop as the weakest link and a site at which drugs can act and disrupt the process of aggregation in mutant carriers.F198S, E200K, V210I and E211Q mutations provide strength to structural configuration mostly in the regions of 165-175. V180I, T183A, T188K, F198Sand E211Q mutants also show improved flexibility in the region around 220-228 which form a part of the C terminus of H3 [34] . So, the ultimate result of MD simulation was that the WT and had the same structural stability [18].

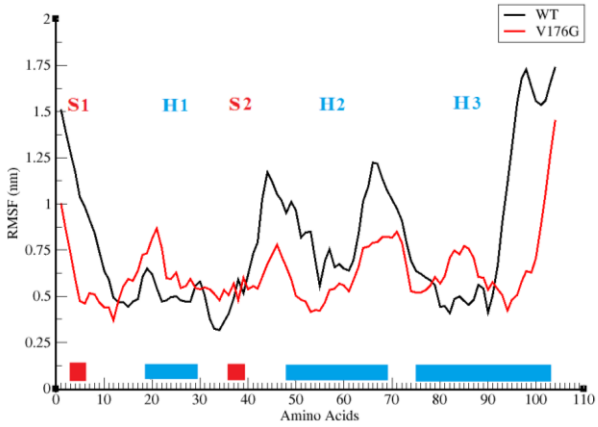

Figure 4 Ca RMSF obtained from the structure of the globular domain (residues 128–225) for PrP mutants (a) wild type, (b) V176G

3.2 Evolution of Secondary Structure

To completely understand the mechanism of production of PrPSc which is the disease causing misfolded protein produced from PrPc which is the normal protein present in human cells and how mutations present in GSS lead to this transformation a thorough study of secondary structure is a must .The breakdown of tertiary structure of prion protein in all the varieties is depicted in Figure 5. It was seen that β-sheet retained its structural configuration for a longer time than H1, H2 and H3 in simulations that studied the mutated variety and WT. The analysis also showed that since H1 has a high affinity towards water, there is greater chance of its disarray and breakdown of the tertiary structure and it has the lowest stability amongst all helices. In WT stimulation it took 4ps [18] to unwind run 1 helices, for run 2, 3 the time was 2ps, along with winding in run 2 and unwinding of β-sheet in run 1, 3. As far as V176G mutation is concerned both H1, H2 in run 1 take 1.25ps to unwind, H3 in run 2 takes 2ps whereas unwinding of H2 in run 3 and change of β-sheet in H3 position with winding β-sheet in both runs 1, 3 needs 0.5ps. The helix undergoes change in structural configuration when the temperature is raised. Analysis showed that the most important factor that helped in disintegrating protein structure was high temperature. The dynamic activity shown by β-sheet was more than that of the helix. Through the simulation based on MD, the lengthening, total and partial unfolding of β-sheet were events that were taking place consistently. As the temperature was raised, the rate of unfolding increased [22]. The low stability of H1 in comparison to H2 and H3 is proved by the accelerated unfolding seen in the simulation [18]. H1 had come out as the helix with the shortest length and at temperature of 523k its structure had broken down completely with increased rate of breakdown at high temperature.

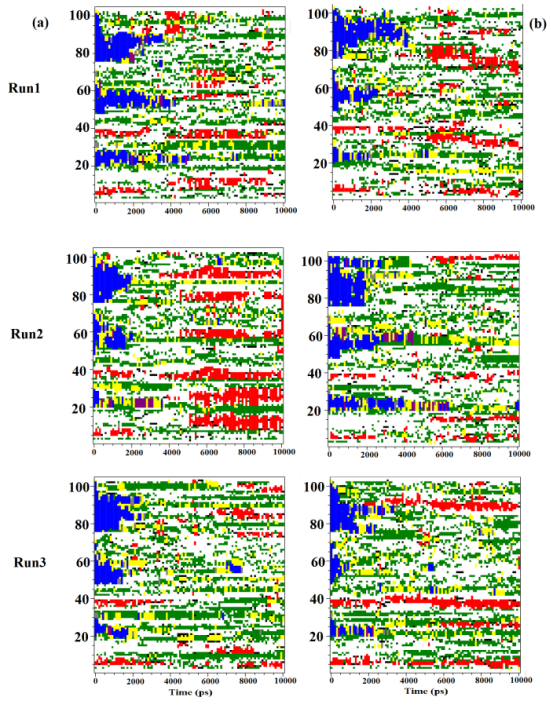

Figure 5 Secondary structure analysis based on the DSSP algorithm for (a) WT, (b) PrP mutant V176G

3.3 Percentage of Secondary Structure

In Table 1 all the components of the secondary structure are enlisted and Figure 6 shows the composition of ß-sheet in WT and V176G, a thorough research on these two showed that increase in mutation was a characteristic feature of misfolded PrP. As far as the mutations were concerned, the elongation of ß-sheet was seen in run 1 and run 3 as determined from the study of secondary structure. In T188R variety of mutation, run 1 and run 2 showed elongation of native ß-sheet which has been documented in previous studies [6]. The percentage of helix in the structural configuration showed a decline as the simulation ran its course. The rate of disintegration of the helix was quite high for D178N variety of mutant. However, rather curiously percentage of β-sheet showed an increase in all these varieties [18]; At temperature of 523k, ß-sheet elongated more rapidly and the total time period needed for elongation of ß-sheet was 492 [22].

Table 1 Average values for the percentage of the secondary structure for WT, V176G mutation

WT SS %	β-sheet	a-helix
0.24	0.07	0.08
0.28	0.15	0.05
0.22	0.05	0.06
Average	**0.09**	**0.06**
V176G SS %	**β-sheet**	**a- helix**
0.25	0.08	0.07
0.23	0.04	0.08
0.23	0.09	0.05
Average	**0.07**	**0.06**

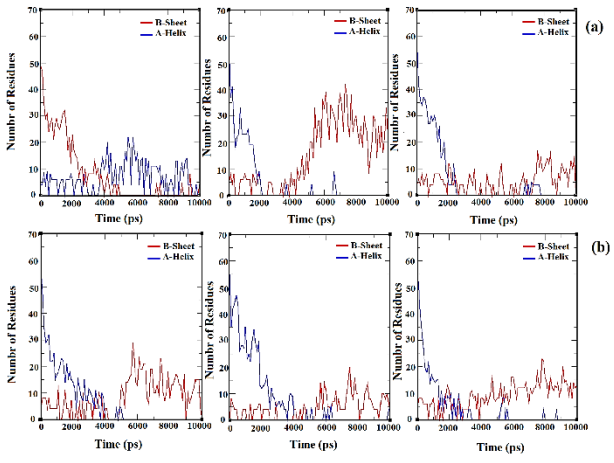

Figure 6 Secondary structure helices (blue) and β-sheets (red) as a function of simulation time determined with DSSP: (a) WT, (b) V176G

3.4 Salt Bridges (SBs)

Sequences adjoining H2, H3 and C terminal of H1 and H3 are interconnected by 7 important salt bridges. The salt bridges are shown in Figure 7 the E211_R208 (SB1), E207_K204 (SB2), E207_R208 (SB3), E200_K204 (SB4), E196_R156 (SB5), E146_K204 (SB6) and D202_R156 (SB7) Figure 7. [1]. The prion structural configuration is such that a greater number of SB present in the structure connecting residues, but the SB's that join together residues located far from each other and interconnect sequences that play important role generally are preserved preferentially [35]. No difference between WT and mutated variety was seen for SB4, SB5and SB7. Even after completion of the simulation salt bridge 4 retained its structure, but salt bridge 5 was totally disintegrated.

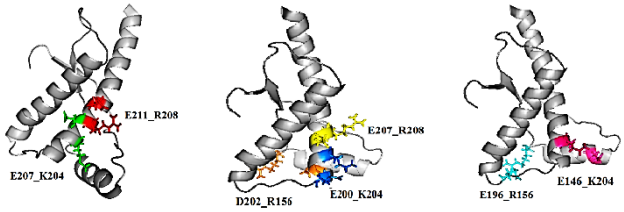

Figure 7 Location of selected SBs on PrP (PDB ID: 1QLX)

The SB4 is enveloped within H3 helical structure and this covering acts as a protective cover against the hazardous impact of mutations Figure 8. SB5 was disintegrated by the mutation confirming its weakest strength among all the salt bridges. Since, it is inherently weak in structure, any mutation can disintegrate it by intramolecular interactions with bonds that have decreased affinity to water having the maximum impact on the region of C- terminal and H2.As seen in simulations conducted in the past in V176G variety of mutation, there was formation of Sb2 salt bridge [36]. SB3, SB6 also is formed in V176G.

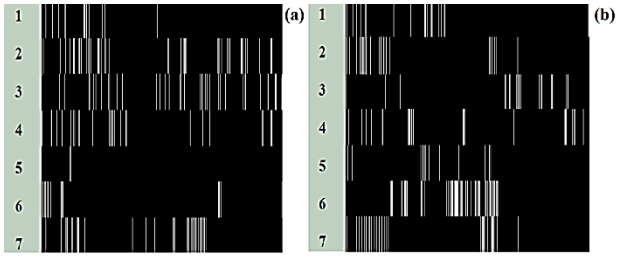

Figure 8 Selected SBs the E211_R208 (1), E207_K204 (2), E207_R208 (3), E200_K204 (4), E196_R156 (5), E146_K204 (6) and D202_R156 (7) involving helices H1, H2 and H3 are plotted over simulation time for all runs. The presence of SBs is indicated as white slits via VMD. (a) WT, (b) PrP mutant V176G

Studies have put forward a theory that mutation flexibility plays an important role in the production of protein form that can cause scrapie and this is

corroborated by the fact that H2 – H3 region has high flexibility [37-40]. The high flexibility of H2 – H3 region is a result of the loss of salt bridges (SB1), either partially or totally [1, 41, 42], proof of this has been seen in in silico studies which demonstrate that the structural folds of H3 and H2 helixes are maintained by interactions between the molecules and the remaining protein structure [38, 43]. All the residues that constitute the SB network are quite similar in all species. If these residues are not present in theirs disintegrated positions then a mutant variety is produced which can cause disease [37], somehow this loop has been found to have greater structural instability in mammals which are victims of prion disease (mouse, sheep and Syrian hamster. When simulations were conducted at a raised temperature and low pH, secondary structure was disintegrated and alteration in tertiary structure was seen. In precise terms misfolding of H2 and disintegration of H2, H3 sequences were seen [44].

3.5 Hydrophobicity and Solvent Accessible Surface Area (SASA)

The determining factor of the strength of the globular domain of PrP, which is made up of a core of side chains that have decreased affinity to water and are constantly interacting with each other is the prion protein which is made of residues. The SASA of the hydrophobic core calculated the following residues Figure 9 Met134, Pro137, Ile139, Phe141, Pro158, Val161, Phe175, Val176, Cys179, Val180, Ile184, Phe198, Val203, Met205, Met206, Val209, Val210, Met213, Cys214, Ile215 [31].The SASA or solvent accessible surface area of the above mentioned core has to be determined to measure the inflexibility as shown in Figure 9. These simulations were conducted on WT and they demonstrated similar results and had SASA values in the last 10ns in case of all proteins and compactness for core, thus proving that all proteins share a similar core WT which has decreased affinity to water. The V176G variety of mutation was evaluated 3 times using simulation and the SASA values obtained were consistently more than WT, the mutation actually changes the relative Solvent Accessible Surface Area thus increasing the chances of interaction of solvent with M205, M206 and M213 as far as weight was concerned.

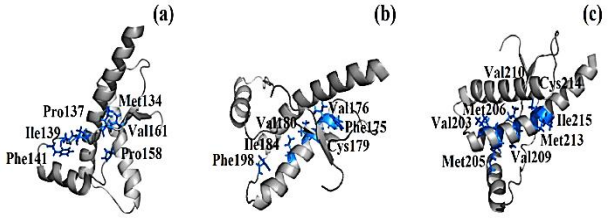

Figure 9 Secondary structure of the prion with the hydrophobic core (a) hydrophobic core at the loop (b) hydrophobic core at the H2 (c) hydrophobic core at the H3

The value of shows in Table 2 the following variation in simulations run 1 (17.4), run 2 (16.8) and in run 3 (18.8), this change is caused by some residue that brings the hydrophobic surface in front. Both environmental factors and the structural configuration of protein can have an impact on the aggregation of PrPSc. The most important factor that has an impact on the collection of monomers is flexibility of the protein and its capacity to be soluble in solvent [45]. Mutations might also uncover the structure of PrP and make it more vulnerable to degradation. D202N and E211 mutants have a higher hydrophobicity than 217R variety and have a higher tendency to self-aggregate if compared to WT [36].

Table 2 Average values for the SASA of the MD trajectories for WT, V176G mutation

WT SASA $(nm)^2$	V176G SASA $(nm)^2$
17.9	17.4
19.5	16.8
18.6	18.8
18.6 **(average)**	17.6 **(average)**

4.0 CONCLUSION

A limited difference between mutant and WT generally, but at some points following such destabilize H1, the observed behaviour in many mutations as well as and also destabilizes of the specific loops in the mutant due to breakdown all of hydrogen Bonds with the formation than in WT as well, The dynamic activity shown by β-sheet was more than that of the helix. In mutation some of the specific salt bridges that proved previously it found in the disease mutants with the disappearance in WT and note there is no Clear change for mutant SASA, hydrophobicity it might be substituted with hydrophobic amino acid (GLY).

Acknowledgement

We are grateful for the UTM grant funding.

References

[1] Rossetti, G., *et al.* 2011. Common Structural Traits Across Pathogenic Mutants Of The Human Prion Protein And Their Implications For Familial Prion Diseases. *Journal of Molecular Biology*. 411(3): 700-712.
[2] Prusiner, S. B., Prions. 1998. *Proceedings of the National Academy of Sciences*. 95(23): 13363-13383.
[3] Caughey, B. W., *et al*. 1991. Secondary structure Analysis of the Scrapie-Associated Protein PrP 27-30 in Water by Infrared Spectroscopy. *Biochemistry*. 30(31): 7672-7680.
[4] Stahl, N., *et al*. 1993. Structural Studies Of The Scrapie Prion Protein Using Mass Spectrometry And Amino Acid Sequencing. *Biochemistry*. 32(8): 1991-2002.
[5] Simpson, M., *et al.* 2013. Unusual Clinical and Molecular-Pathological Profile of Gerstmann-Sträussler-Scheinker Disease Associated With a Novel PRNP Mutation (V176G). *JAMA Neurology*. 70(9): 1180-1185.

[6] Guo, J., *et al.* 2012. Influence of the Pathogenic Mutations T188K/R/A on the structural Stability And Misfolding Of Human Prion Protein: Insight From Molecular Dynamics Simulations. *Biochimica et Biophysica Acta (BBA)-General Subjects.* 1820(2): 116-123.
[7] Prusiner, S. B. 1994. Inherited Prion Diseases. *Proceedings of the National Academy of Sciences of the United States of America*. 91(11): 4611.
[8] Liemann, S. and R. Glockshuber. 1999. Influence of Amino Acid Substitutions Related To Inherited Human Prion Diseases On The Thermodynamic Stability Of The Cellular Prion Protein. *Biochemistry.* 38(11): 3258-3267.
[9] Swietnicki, W., *et al*. 1998. Familial Mutations And The Thermodynamic Stability Of The Recombinant Human Prion Protein. *Journal of Biological Chemistry*. 273(47): 31048-31052.
[10] Apetri, A. C., K. Surewicz, and W. K. Surewicz. 2004. The Effect Of Disease-Associated Mutations On The Folding Pathway Of Human Prion Protein. *Journal of Biological Chemistry*. 279(17): 18008-18014.
[11] Horiuchi, M. and B. Caughey. 1999. Prion Protein Interconversions And The Transmissible Spongiform Encephalopathies. *Structure.* 7(10): R231-R240.
[12] Biasini, E., *et al.* 2008. Multiple Biochemical Similarities Between Infectious And Non-Infectious Aggregates Of A Prion Protein Carrying An Octapeptide Insertion. Journal of neurochemistry, 104(5): 1293-1308.
[13] Jeffrey, M., *et al.* 2009. Prion Protein with an Insertional Mutation Accumulates on Axonal and Dendritic Plasmalemma and is Associated with Distinctive Ultrastructural Changes. *The American Journal Of Pathology*. 175(3): 1208-1217.
[14] Brown, K. and J. A. Mastrianni. 2010. The Prion Diseases. *Journal of Geriatric Psychiatry And Neurology*. 23(4): 277-298.
[15] Jeong, B.-H. and Y.-S. Kim. 2014. Genetic Studies in Human Prion Diseases. *Journal of Korean Medical Science*. 29(5): 623-632.
[16] Chara, O., J.R. Grigera, and A. N. McCarthy. 2007. Studying the Unfolding Kinetics Of Proteins Under Pressure Using Long Molecular Dynamic Simulation Runs. *Journal Of Biological Physics*. 33(5-6): 515-522.
[17] Perezzan, R. and A. Rey. 2012. Simulating Protein Unfolding Under Pressure With A Coarse-Grained Model. *The Journal Of Chemical Physics.* 137(18): 185102.
[18] Shamsir, M. S. and A. R. Dalby. 2005. One Gene, Two Diseases And Three Conformations: Molecular Dynamics Simulations Of Mutants Of Human Prion Protein At Room Temperature And Elevated Temperatures. *Proteins: Structure, Function, and Bioinformatics.* 59(2): 275-290.
[19] Wang, T. and R. C. Wade. 2007. On the Use Of Elevated Temperature In Simulations To Study Protein Unfolding Mechanisms. *Journal of Chemical Theory and Computation*. 3(4): 1476-1483.
[20] Tran, H. T., A. Mao, and R. V. Pappu. 2008. Role of Backbone−Solvent Interactions in Determining Conformational Equilibria of Intrinsically Disordered Proteins. *Journal of the American Chemical Society*. 130(23): 7380-7392.
[21] Lindorff-Larsen, K., *et al.* 2011. How Fast-Folding Proteins Fold. Science. 334(6055): 517-520.
[22] Chen, X., *et al.* 2013. Molecular Dynamics Simulation Of Temperature Induced Unfolding Of Animal Prion Protein. Journal Of Molecular Modeling. 19(10): 4433-4441.
[23] Rossetti, G., *et al*. 2010. Structural Facets Of Disease-Linked Human Prion Protein Mutants: A Molecular Dynamic Study. *Proteins: Structure, Function, and Bioinformatics*. 78(16): 3270-3280.
[24] Hess, B., *et al*. 2008. GROMACS 4: Algorithms For Highly Efficient, Load-Balanced, And Scalable Molecular Simulation. *Journal Of Chemical Theory And Computation*. 4(3): 435-447.
[25] Nose, S. and M. Klein. 1983. Constant Pressure Molecular Dynamics For Molecular Systems. *Molecular Physics.* 50(5): 1055-1076.
[26] Nosé, S. 1984. A Molecular Dynamics Method For Simulations In The Canonical Ensemble. *Molecular Physics.* 52(2): 255-268.
[27] Hoover, W. G. 1985. Canonical Dynamics: Equilibrium Phase-Space Distributions. *Physical Review A*. 31(3): 1695.
[28] Darden, T., D. York, and L. Pedersen. 1993. Particle Mesh Ewald: An N· Log (N) Method For Ewald Sums In Large Systems. *The Journal Of Chemical Physics.* 98(12): 10089-10092.
[29] Kabsch, W. and C. Sander. 1983. Dictionary Of Protein Secondary Structure: Pattern Recognition Of Hydrogen-Bonded And Geometrical Features. *Biopolymers.* 22(12): 2577-2637.
[30] Humphrey, W., A. Dalke, and K. Schulten. 1996. VMD: Visual Molecular Dynamics. *Journal Of Molecular Graphics.* 14(1): 33-38.
[31] Van der Kamp, M. W. and V. Daggett. 2010. Influence Of Ph On The Human Prion Protein: Insights Into The Early Steps Of Misfolding. *Biophysical Journal*. 99(7): 2289-2298.
[32] Viles, J. H., *et al.* 2001. Local Structural Plasticity Of The Prion Protein. Analysis Of NMR Relaxation Dynamics. Biochemistry. 40(9): 2743-2753.
[33] O'Sullivan, D. B., *et al.* 2009. Dynamics Of A Truncated Prion Protein, Prp (113–231), From 15N NMR Relaxation: Order Parameters Calculated And Slow Conformational Fluctuations Localized To A Distinct Region. *Protein Science*.18(2): 410-423.
[34] Meli, M., M. Gasset, and G. Colombo. 2011. Dynamic Diagnosis Of Familial Prion Diseases Supports The B2-A2 Loop As A Universal Interference Target. *PLoS One*. 6(4): e19093.
[35] Donald, J. E., D. W. Kulp, and W. F. DeGrado. 2011. Salt Bridges: Geometrically Specific, Designable Interactions. *Proteins: Structure, Function, and Bioinformatics.* 79(3): 898-915.
[36] Guo, J., *et al*. 2012. Exploring structural And Thermodynamic Stabilities Of Human Prion Protein Pathogenic Mutants D202N, E211Q and Q217R. *Journal Of Structural Biology*. 178(3): 225-232.
[37] Adrover, M., et al. 2010. Prion Fibrillization Is Mediated By A Native Structural Element That Comprises Helices H2 and H3. *Journal of Biological Chemistry*. 285(27): 21004-21012.
[38] Kallberg, Y., *et al.* 2001. Prediction Of Amyloid Fibril-Forming Proteins. *Journal of Biological Chemistry*. 276(16): 12945-12950.
[39] Tartaglia, G. G., *et al.* 2008. Prediction of Aggregation-Prone Regions In Structured Proteins. *Journal Of Molecular Biology*. 380(2): 425-436.
[40] Chakroun, N., *et al.* 2010. The oligomerization Properties Of Prion Protein Are Restricted To The H2H3 Domain. *The FASEB Journal.* 24(9): 3222-3231.
[41] Bamdad, K. and H. Naderi-Manesh. 2007. Contribution Of A Putative Salt Bridge And Backbone Dynamics In The Structural Instability Of Human Prion Protein Upon R208H Mutation. Biochemical And Biophysical Research Communications. 364(4): 719-724.
[42] Zhang, Y., *et al.* 2006. Molecular Dynamics Study On The Conformational Transition Of Prion Induced By The Point Mutation: F198S. *Thin Solid Films.* 499(1): 224-228.
[43] Kimura, T., *et al*. 2011. Synthesis of GN8 Derivatives And Evaluation Of Their Antiprion Activity In TSE-Infected Cells. *Bioorganic & Medicinal Chemistry Letters.* 21(5): 1502-1507.
[44] Rossetti, G., S. Bongarzone, and P. Carloni. 2013. Computational Studies On The Prion Protein. *Current Topics In Medicinal Chemistry.* 13(19): 2419-2431.
[45] Chong, S.-H., *et al.* 2011. Structural And Thermodynamic Investigations On The Aggregation And Folding Of Acylphosphatase By Molecular Dynamics Simulations And Solvation Free Energy Analysis. *Journal of the American Chemical Society*. 133(18): 7075-7083.